Toward isotope-aware RMP modeling: integral FLR ions and turbulence in electron screening currents

M.J. Markl[1], S.V. Kasilov[1,2], J. Schatzlmayr[1], C.G. Albert[1],
and the EUROfusion Tokamak Exploitation Team*

[1] *Fusion@ÖAW, Institute of Theoretical and Computational Physics, Graz University of Technology, Petersgasse 16, 8010 Graz, Austria*
[2] *Institute of Plasma Physics, National Science Center "Kharkov Institute of Physics and Technology", 61108 Kharkiv, Ukraine*
* *See the author list of N. Vianello et al 2026 Nucl. Fusion 66 116010*

Introduction

ITER will operate in high confinement mode, where edge localized modes (ELMs) threaten wall component lifetime and make reliable ELM control a prerequisite for safe operation. A leading method applies small resonant magnetic perturbations (RMPs, $\delta B/B_0 \approx 10^{-4}$), keeping the edge pressure gradient below the ELM stability limit. Near rational surfaces the plasma responds with localized parallel currents that screen the RMP. Under suitable density and rotation this shielded state bifurcates to a penetrated one near the pedestal top, correlating with the onset of ELM suppression [1, 2]. Necessary conditions for suppression are established in deuterium [3] but remain unclear in mixed-isotope plasmas. In ASDEX Upgrade, adding hydrogen to a suppressed deuterium plasma reverts it to ELM mitigation once the hydrogen fraction reaches about 40% [4]. Whether tritium behaves likewise is an open, ITER-relevant question.

We study the screening response with the integral linear kinetic code KIM [5], the finite-Larmor-radius (FLR) expansion code FLR2 [6], and the δf Monte-Carlo guiding-centre orbit tracing code GORILLA [7]. Their small Larmor radius makes electrons well described to leading FLR order (drift-kinetic approximation), whereas ions are not. Resolving the ion Larmor radius to all orders is required, as the second-order expansion of FLR2 produces unphysical modes absent in KIM [5]. The linear response further proves electron-dominated and essentially isotope-independent, so it cannot by itself explain the loss of suppression in deuterium–hydrogen plasmas. This points to turbulence on the current-carrying electrons as the missing, isotope-sensitive ingredient, for which GORILLA provides the natural platform. We report progress on this development.

Integral kinetic response in a cylinder: KIM and FLR2

In the large-aspect-ratio limit with circular cross-section we model the plasma as a cylindrical, inhomogeneous column with a helical field, that is effectively one-dimensional in the radius r. We consider the linearised electrostatic problem in a proper FLR treatment by representing the perturbed charge density through integral kernels acting on the field perturbations,

$$\delta\rho(r) = \int \mathrm{d}r'\, K^{\rho\Phi}(r,r')\,\delta\Phi(r') + \int \mathrm{d}r'\, K^{\rho B}(r,r')\,\delta B^r(r'), \tag{1}$$

where δB^r ($\delta\Phi$) is the radial magnetic field (electrostatic potential) perturbation. The kernels are velocity moments of the perturbed distribution function from the linearized kinetic equation, solved by a Fourier-series ansatz in action–angle variables with an energy-preserving Ornstein–Uhlenbeck collision operator, following the local model of [8] and derived fully in [5]. Dis-

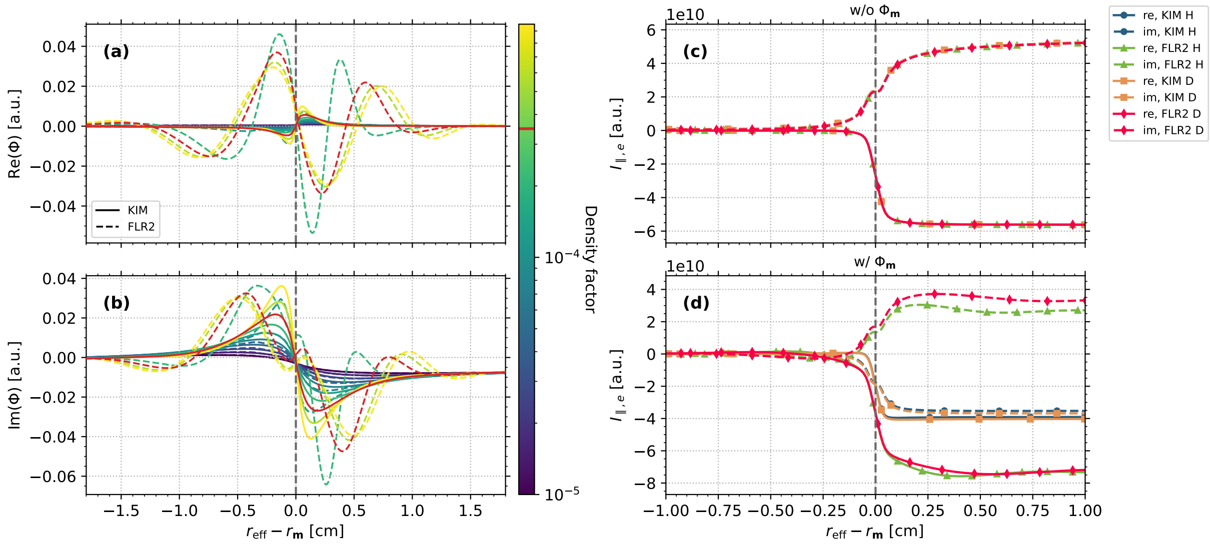

Figure 1: KIM-FLR2 comparison for AUG 33353 and mode $\mathbf{m} = (m,n) = (6,2)$, reproduced from [5] (which uses the same data discussed in [2]). (a,b) Real and imaginary parts of the electrostatic potential Φ through the density-rescaling fade-in of FLR effects (KIM solid, FLR2 dashed; colour encodes the density factor, the red curve marks the onset of FLR relevance). (c,d) Integrated electron screening current $I_{\parallel,e}$ from KIM and FLR2 for hydrogen and deuterium (real solid, imaginary dashed), (c) without and (d) with the electrostatic potential perturbation harmonic $\Phi_{\mathbf{m}}$.

cretizing Poisson's equation with finite elements yields a linear system for $\delta\Phi$, from which the screening current $\delta j_\parallel$ follows through two further kernels.

KIM evaluates the kernels without expansion, capturing the ion Larmor radius to all orders. FLR2 [6] instead Taylor-expands them to second order, reducing the integral relation to a local, differential one. The expansion is controlled by $|k_\perp|\rho_{T\sigma}$, with thermal Larmor radius $\rho_{T\sigma} = v_{T\sigma}/\omega_{c\sigma} \propto \sqrt{m_\sigma}$. For electrons $|k_\perp|\rho_{Te} \ll 1$ holds broadly, but KIM shows it breaks down for ions even near the resonant surface [5]. Isotope dependence enters here solely through $\rho_{T\sigma}$.

For vanishing FLR contributions ($\rho_{T\sigma}/\lambda_D \ll 1$, large Debye length) KIM and FLR2 agree. Reducing λ_D fades the FLR terms in, and once $|k_\perp|\rho_{T\sigma} \gtrsim 1$ FLR2 develops strong potential oscillations whereas KIM stays smooth and converges to the quasineutrality solution (Fig. 1a,b) [5]. These oscillations are an artefact, arising once the mode wavelength drops below the ion Larmor radius, to which the integral KIM treatment is immune.

The artefacts distort the screening current. Without the potential the two codes' electron current agrees. With $\delta\Phi$ included, the broad spurious FLR2 potential multiplies the narrow (1–2 mm) electron susceptibility layer and only weakly perturbs the current, whereas in KIM a comparably narrow potential reinforces it and even reverses the sign of the imaginary part (Fig. 1c,d). The integrated shielding current is consequently larger in FLR2 than in KIM, so the integral treatment matters for penetration estimates.

Turning to isotopes, the ion kernel depends on mass only through $\rho_{T\sigma} \propto \sqrt{m_\sigma}$, marginal for the deuterium/hydrogen mass ratio of two. As the shielding is electron-dominated, the KIM response is essentially identical for the two isotopes. FLR2, by contrast, shows a spurious isotope dependence inherited from its mass-dependent artefacts [5]. The proper ion FLR treatment is

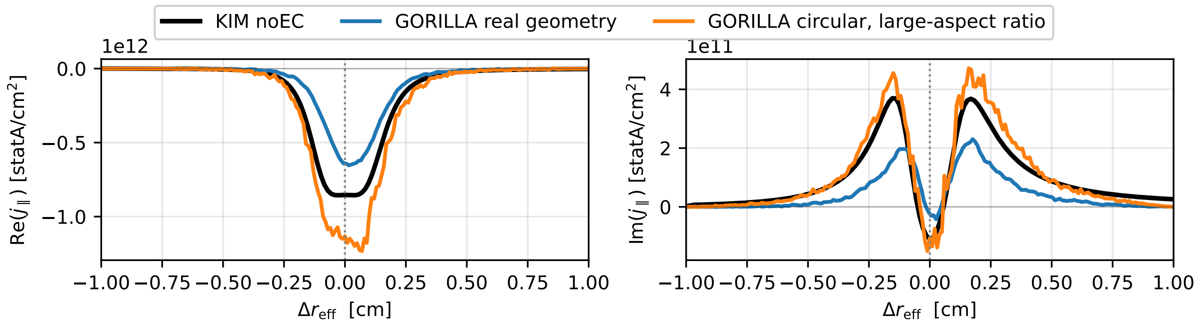

Figure 2: Benchmark of screening current densities in KIM and GORILLA, the latter in real geometry and in the circular cross-section large aspect ratio limit.

thus necessary for accuracy, but the linear response does not account for the isotope effect.

δf Monte-Carlo screening current and turbulent broadening: GORILLA

We compute the dominant electron screening current with the guiding-center orbit code GORILLA [7] in a δf Monte-Carlo scheme, using data from ASDEX Upgrade discharge 33353. The single helical $(m,n) = (7,2)$ perturbation is carried by a time-dependent marker weight $w(t)$ [9], with $\delta f = w f_{\mathrm{Maxwell}}$, whose evolution contains the radial magnetic field perturbation,

$$\frac{\mathrm{d}w}{\mathrm{d}t} + \nu_r w = -\delta v_g^r \left(A_1 + A_2 \frac{mv^2}{2T} \right), \qquad \delta v_g^r = v_\parallel \frac{\delta B^r}{B_0}, \tag{2}$$

with thermodynamic forces $A_{1,2}$ (as defined in [2]) and a regularization rate ν_r being much smaller than collision frequency. Further, an Ornstein-Uhlenbeck operator (without energy conservation) provides the collisions. The parallel screening current then follows as

$$\delta j_\parallel(\mathbf{r}) \approx \frac{ZenV_W}{N} \sum_k w_k v_{\parallel k} \delta(\mathbf{r} - \mathbf{r}_k), \tag{3}$$

over the N markers, with V_W the sampling volume. In practice, Eq. (3) is evaluated as a box and time average over the marker orbit history, taken much longer than the regularization time $1/\nu_r$, which is itself chosen larger than the decorrelation time, so the averaging window far exceeds the decorrelation time. Following true guiding centre orbits in actual geometry, GORILLA needs no cylindrical reduction. Nevertheless, in the circular cross-section large aspect ratio limit, GORILLA reproduces a similar screening current density than KIM (omitting energy conservation) as shown in figure 2.

Since the linear response is electron-dominated and isotope-blind, the isotope effect likely enters through turbulence acting on the current-carrying electrons. As a first realisation, we include this turbulence crudely as a random spatial displacement consistent with a prescribed constant diffusion coefficient D_a, where $D_a = 9.2 \cdot 10^3$ cm^2/s for deuterium [2]. Also, to mimic the misalignment electric field that was shown in [2] to drive shielding currents, we set δB^r as a rectangular function with 1 G in a $\pm$ 0.1 cm region around the resonant surface and zero otherwise. Figure 3a,b shows that anomalous diffusion broadens the resonance layer and simultaneously weakens the amplitude. Rescaling the anomalous coefficient according to gyroBohm

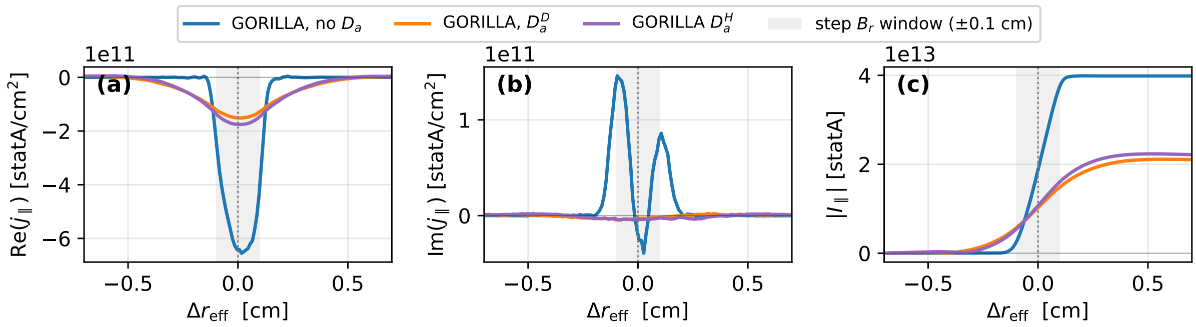

Figure 3: Comparison of (a-b) screening current density and (c) integrated current calculated in GORILLA with and without anomalous diffusion.

scaling ($D^a \propto \sqrt{m_i}$) provides an estimate for hydrogen. Notably, the integrated current in figure 3c indicates a clear turbulence-decreased shielding, yet overall no significant isotope dependence due to the crudeness of the turbulence estimate. Nevertheless it provides a first step toward a quantitative treatment of the missing physics.

Summary and outlook

We have set out an integral and turbulent approach to the kinetic plasma response underlying RMP ELM suppression. The integral code KIM resolves the ion Larmor radius to all orders and removes the unphysical modes of the second-order expansion FLR2. The resulting linear response is electron-dominated and nearly isotope-independent, and so cannot explain the loss of suppression in deuterium–hydrogen plasmas. The δf code GORILLA supplies an independent, geometry-faithful benchmark and, by admitting turbulence effects on the electron orbits. Though, the present crude turbulence model is not capable of properly resolving the isotope dependence, it provides a route to the isotope-sensitive physics the linear response omits. Future work will develop the turbulence estimate toward a quantitative isotope dependence and couple GORILLA to the hybrid-MHD-kinetic toroidal code MEPHIT [6].

Acknowledgements

This work has been carried out within the framework of the EUROfusion Consortium, funded by the European Union via the Euratom Research and Training Programme (Grant Agreement No 101052200 — EUROfusion). Views and opinions expressed are however those of the author(s) only and do not necessarily reflect those of the European Union or the European Commission. Neither the European Union nor the European Commission can be held responsible for them.

References

[1] Q.M. Hu et al. In: Nucl. Fusion, 2020, **60**, (7), 076001.
[2] M. Markl et al. In: Nucl. Fusion, 2023, **63**, (12), 126007.
[3] W. Suttrop et al. In: Nucl. Fusion, 2018, **58**, (9), 096031.
[4] N. Leuthold et al. In: Nucl. Fusion, 2024, **64**, (2), 026017.
[5] M. J. Markl et al. In: submitted to Journal of Plasma Physics, 2026.
[6] P Lainer et al. In: Plasma Physics and Controlled Fusion, 2026, **68**, (5), 055037.
[7] M. Eder et al. In: Journal of Open Source Software, 2023, **8**, (86), 4890.
[8] M. F. Heyn et al. In: Nucl. Fusion, 2014, **54**, (6), 064005.
[9] C G Albert et al. In: J. Phys.: Conf. Ser. 2016, **775**, 012001.